# Plethora of transitions during breakup of liquid filaments

José Rafael Castrejón-Pita[a], Alfonso Arturo Castrejón-Pita[b], Sumeet Suresh Thete[c], Krishnaraj Sambath[c], Ian M. Hutchings[a], John Hinch[d], John R. Lister[d], and Osman A. Basaran[c,1]

[a]Department of Engineering, University of Cambridge, Cambridge CB3 0FS, United Kingdom; [b]Department of Engineering Science, University of Oxford, Oxford OX1 3PJ, United Kingdom; [c]School of Chemical Engineering, Purdue University, West Lafayette, IN 47907-1283; and [d]Department of Applied Mathematics and Theoretical Physics, University of Cambridge, Cambridge CB3 0WA, United Kingdom

Thinning and breakup of liquid filaments are central to dripping of leaky faucets, inkjet drop formation, and raindrop fragmentation. As the filament radius decreases, curvature and capillary pressure, both inversely proportional to radius, increase and fluid is expelled with increasing velocity from the neck. As the neck radius vanishes, the governing equations become singular and the filament breaks. In slightly viscous liquids, thinning initially occurs in an inertial regime where inertial and capillary forces balance. By contrast, in highly viscous liquids, initial thinning occurs in a viscous regime where viscous and capillary forces balance. As the filament thins, viscous forces in the former case and inertial forces in the latter become important, and theory shows that the filament approaches breakup in the final inertial–viscous regime where all three forces balance. However, previous simulations and experiments reveal that transition from an initial to the final regime either occurs at a value of filament radius well below that predicted by theory or is not observed. Here, we perform new simulations and experiments, and show that a thinning filament unexpectedly passes through a number of intermediate transient regimes, thereby delaying onset of the inertial–viscous regime. The new findings have practical implications regarding formation of undesirable satellite droplets and also raise the question as to whether similar dynamical transitions arise in other free-surface flows such as coalescence that also exhibit singularities.

inertial | viscous | capillary | scaling | regimes

**D**rop formation is ubiquitous in daily life, industry, and nature (1–3). The phenomenon is central to inkjet printing (4, 5), dripping from leaky faucets (6, 7), measurement of equilibrium and dynamic surface tension (8, 9), DNA arraying and printing of cells (10, 11), chemical separations and analysis (12, 13), production of particles and capsules (14, 15), printing of wires and transistors (16, 17), and mist formation in waterfalls and fragmentation of raindrops (18, 19). Fig. 1A shows an experimental setup for studying the dynamics of a drop of an incompressible Newtonian fluid of density $\rho$, viscosity $\mu$, and surface tension $\sigma$ forming from a tube of radius $R$ (Fig. 1B and *Drop Formation from a Tube and Filament Thinning*). A salient feature of, and key to understanding, drop formation is the occurrence of a thin filament that connects an about-to-form primary drop to the rest of the fluid that is attached to the tube (Fig. 1 B and C). Thus, it often proves convenient to study filament thinning in the idealized setup depicted in Fig. 1D (*Drop Formation from a Tube and Filament Thinning*). As time $t$ advances and the filament radius decreases, curvature and capillary pressure, both of which are at leading order inversely proportional to radius, increase and fluid is expelled with increasing velocity from the neck. At the instant $t = t_b$ when the neck radius vanishes, a finite time singularity occurs and the filament breaks. When the filament breaks, one or more satellite droplets may also form. These satellites are typically much smaller than the primary drop (20) and almost always undesirable in applications (2).

For Newtonian filaments, three theories have been developed to describe the dynamics in the vicinity of the pinch-off singularity (*Scaling Theories of Pinch-Off*). When viscous effects are weak, thinning and pinching occur in an inertial (I) regime (21–23) where inertial and capillary forces balance, and the minimum filament radius $h_{min}$ (Fig. 1B) and the instantaneous Reynolds number $Re(t)$ vary with dimensionless time $\tau$ to breakup as

$$\frac{h_{min}}{R} \sim \tau^{2/3}, \quad Re(t) \sim \frac{1}{Oh}\tau^{1/3}, \qquad [1]$$

where $\tau \equiv (t_b - t)/t_I$ and $t_I \equiv \sqrt{\rho R^3/\sigma}$ (*Scaling Theories of Pinch-Off*). For real liquids, the Ohnesorge number $Oh = \mu/\sqrt{\rho R \sigma}$ is not identically zero no matter how small the viscosity. Thus, for low-viscosity liquids, $Oh \ll 1$ and Eq. 1 shows that regardless of how large the Reynolds number is initially, as $\tau \to 0$ and breakup is approached, $Re(t) \to 0$. Therefore, the inertial regime cannot persist all of the way to breakup and can only describe the initial dynamics for low-viscosity fluids. Similarly, when viscous effects are dominant, thinning and pinching occur in a viscous (V) regime (24) where viscous and capillary forces balance, and $h_{min}$ and $Re(t)$ vary with $\tau$ as

$$\frac{h_{min}}{R} \sim \tau, \quad Re(t) \sim \frac{1}{Oh^2}\tau^{2\beta-1}, \qquad [2]$$

where $\tau \equiv (t_b - t)/t_V$, $t_V \equiv \mu R/\sigma$, and $\beta = 0.175$ (*Scaling Theories of Pinch-Off*). For real liquids, $Oh$ cannot be infinite no matter how large the viscosity. Thus, for high-viscosity liquids, $Oh \gg 1$ and

## Significance

Fluid flows, governed by nonlinear equations, permit formation of singularities. Often, singularities are artifacts of neglecting physical effects. However, free-surface flows exhibit observable singularities including filament pinch-off. As filaments thin, slightly (highly) viscous filaments are expected from theory to transition from an inertial (viscous) regime where viscosity (density) is negligible to an inertial–viscous regime where viscous and inertial effects are important. Previous works show this transition either does not occur or occurs for filament radii well below theoretical predictions. We demonstrate that thinning filaments unexpectedly pass through a number of intermediate transient regimes, thereby delaying onset of the final regime. The findings raise the question if similar dynamical transitions arise in problems that are not necessarily hydrodynamic in nature.
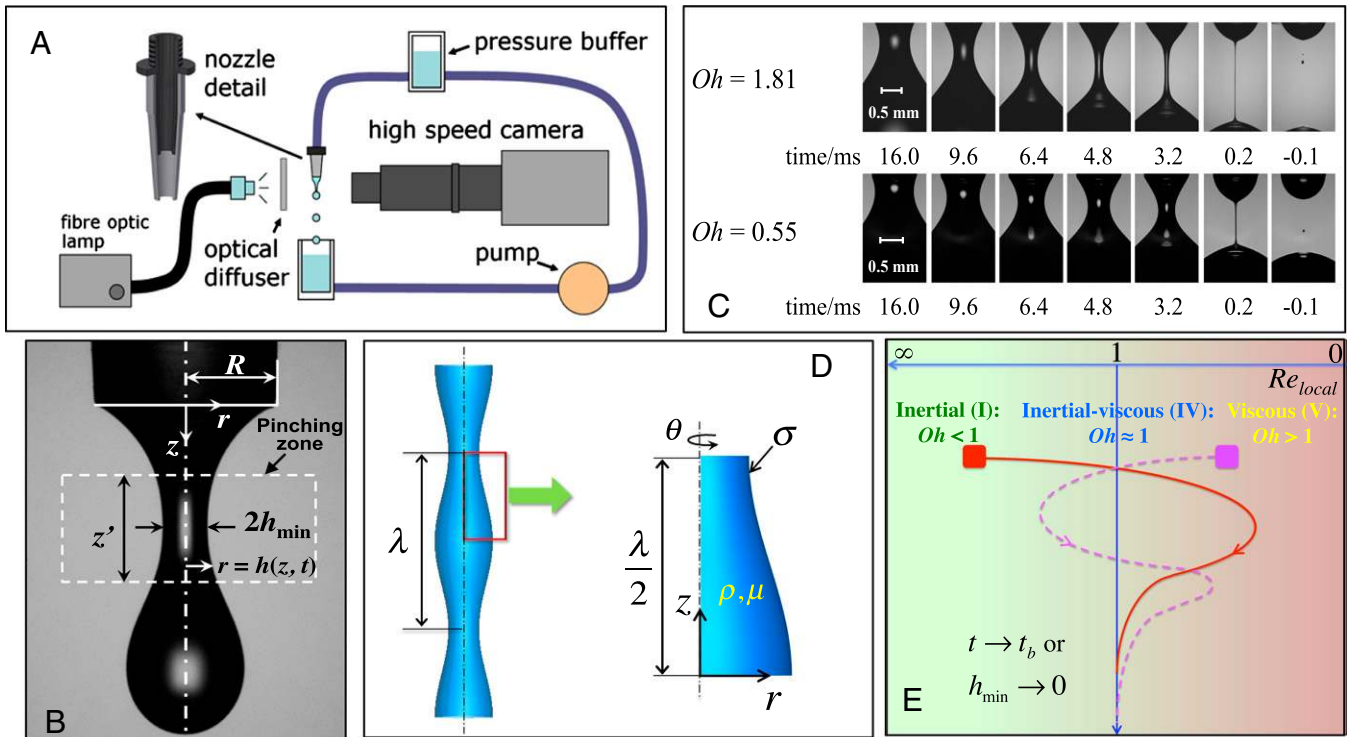
**Fig. 1.** Methods used for studying and new phase diagram for capillary thinning and pinch-off. (*A*) Experimental setup used to capture images of the thinning neck of a drop forming from a nozzle. The images are then postprocessed to obtain the minimum neck radius as a function of the time remaining until breakup. (*B*) Snapshot of a drop forming from a tube that highlights the pinching zone in the vicinity of the pinch point. (*C*) Two series of images that focus on the pinching zones and depict the evolution in time of thinning filaments for drops of two fluids with different viscosities (i.e., different *Oh*). (*D*) Setup for simulating filament thinning and pinch-off: periodically perturbed jet (*Left*) and domain of axial length $\lambda/2$ used in simulations (*Right*). (*E*) Phase space showing trajectories taken by filaments of a slightly viscous (*Oh* < 1) and a highly viscous (*Oh* > 1) fluid. The large squares indicate the starting states at $t = 0$. The arrows along each trajectory show the direction of evolution.

Eq. 2 shows that regardless of how small the Reynolds number is initially, as $\tau \to 0$ and breakup is approached, $Re(t) \to \infty$. Therefore, the V regime cannot persist all of the way to breakup and hence can only describe the initial dynamics even for high-viscosity fluids. Therefore, as the filament radius tends to zero, a transition occurs from either the I or the V regime to a final inertial–viscous (IV) regime in which all three forces, i.e., inertial, viscous, and capillary, balance and the instantaneous Reynolds number $Re(t) \sim 1$ (25). From Eqs. 1 and 2, the transition from the I to the IV regime and that from the V to IV regime can be calculated by setting $Re(t)$ to be order one. Thus, transition from the I to the IV regime should occur when (2, 18)

$$h_{min}/R \sim Oh^2, \qquad [3]$$

and that from the V to the IV regime should occur when (2, 18)

$$h_{min}/R \sim Oh^{2/(2\beta-1)}. \qquad [4]$$

However, whereas careful simulations and experiments have shown that the transition from the I to the IV regime does indeed occur, it has been found to take place for values of $h_{min}$ that are about an order of magnitude smaller than that predicted from theory (Eq. **3**) (26). Furthermore, the transition from the V to the IV regime has not yet been demonstrated to occur from simulation and an attempt for an experimental demonstration of the transition (27) was perhaps at too small a value of *Oh* (*Oh* = 0.49) to be conclusively in the V regime. In this paper, we demonstrate that in contrast with the conventional wisdom that the dynamics of capillary pinching should exhibit a transition from either the I to the IV regime or the V to the IV regime, the

transition from either of the two initial regimes to the final IV regime is in fact more complex and, unexpectedly, can be delayed by the occurrence of a number of intermediate transient regimes as shown in Fig. 1*E*. The possibility of such complexity has been anticipated in part by Eggers (18) but no study has yet been carried out to explore the existence of these intermediate regimes or contemplate its implications in other free-surface flows exhibiting finite time singularities.

In this work, the dynamics of filament thinning is studied both numerically and experimentally. Simulations are performed to track how sinusoidal perturbations on a liquid cylinder cause it to break, which have been successfully used in the past to study pinch-off and scaling for Newtonian (26, 28) as well as non-Newtonian fluids (29, 30) (Fig. 1*D* and *Simulations*). In the experiments, high-speed imaging and image analysis are used to measure the evolution in time of the minimum filament radius for liquids dripping from a tubular nozzle. Glycerol–water mixtures are used as working fluids to explore systems with different values of *Oh*.

Fig. 2*A* shows the computed variation of $h_{min}$ with $\tau$ for a slightly viscous liquid of *Oh* = 0.23. The simulations make plain that after sufficient time has passed so that the initial transients have decayed, the filament first thins in the I regime, where $h_{min} \sim \tau^{2/3}$, as expected. According to conventional wisdom, the thinning dynamics is expected to transition from the I regime to the IV regime when $h_{min} \sim Oh^2 = 0.053$; thenceforward, the thinning is to follow IV scaling where $h_{min} = 0.0304\tau/Oh$. However, the simulation results show that this transition is delayed and does not take place until $h_{min}$ has fallen below a value that is about an order of magnitude smaller than that predicted by the theoretical estimate. Moreover, the simulations show unexpectedly
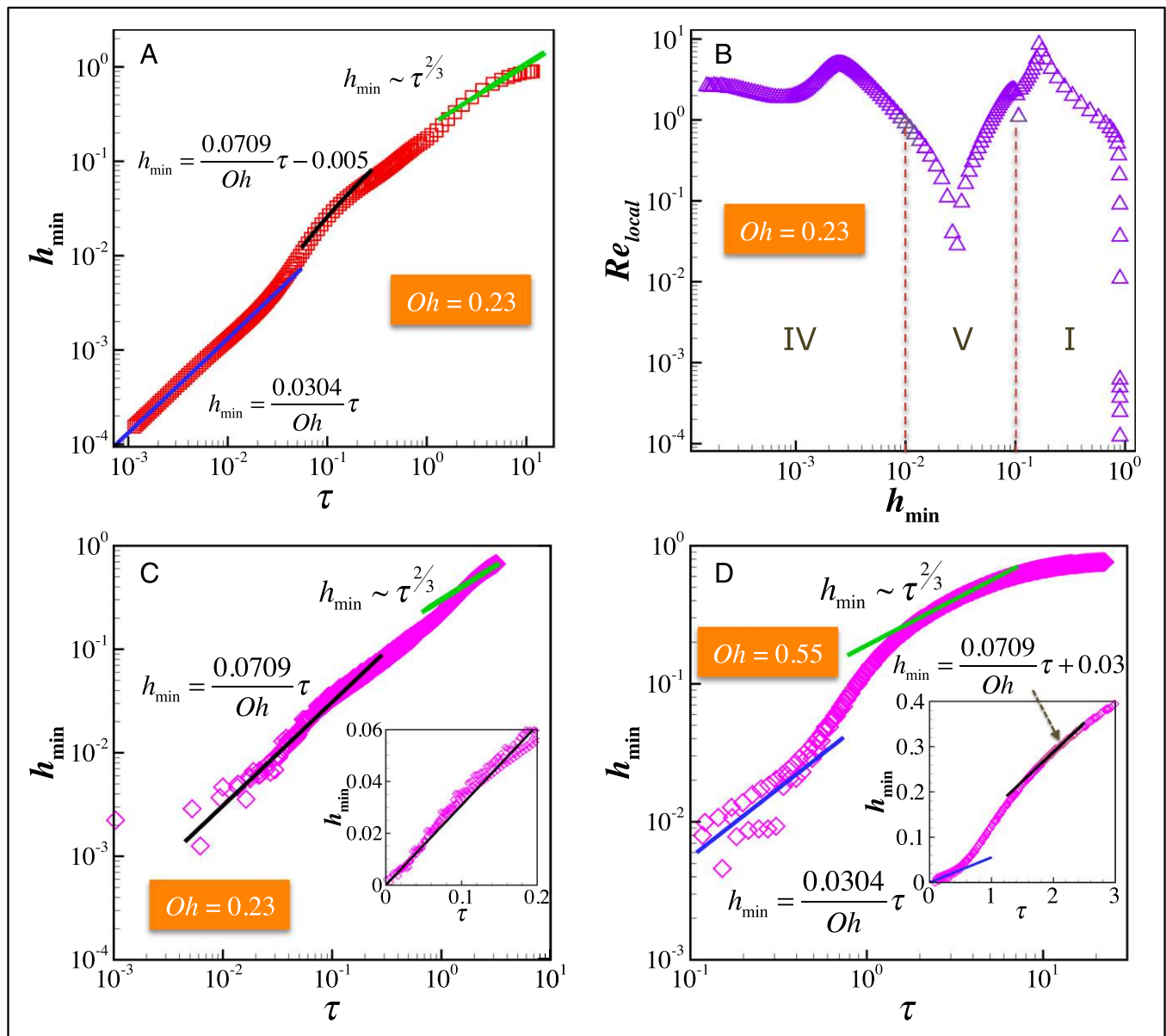
**Fig. 2.** Simulations and experiments demonstrating the existence of an intermediate viscous regime between the initial inertial regime and the final IV regime for slightly viscous fluids ($Oh < 1$). (*A*) Variation of minimum neck radius with time until breakup when $Oh = 0.23$ obtained from simulations. (*B*) Computed variation with minimum neck radius of the local Reynolds number in the neighborhood of the pinch point verifies the existence of all three regimes: $Re_{local} \gg 1$ in the I regime, $Re_{local} \ll 1$ in the V regime, and $Re_{local} \sim 1$ in the IV regime. (*C*) Experimental confirmation of the existence of an intermediate V regime when $Oh = 0.23$. The IV regime is not attained here because of optical limitations. (*D*) At a slightly higher value of $Oh$ than that in C ($Oh = 0.55$), the V to IV transition is observed experimentally. (*C* and *D*, *Insets*) Same data as in the main figures are presented but use linear rather than logarithmic axes.

that the dynamics switches over from the I to the IV regime only after passing through an intermediate V regime, where $h_{min} = 0.0709\tau/Oh$. The existence of these regimes can be verified by plotting the local Reynolds number $Re_{local}$ (*Simulations*) in the thinning filament in the vicinity of the pinch point as a function of $h_{min}$ (Fig. 2*B*). Fig. 2*B* clearly shows that at early times when $h_{min} \approx 0.2$, $Re_{local} \gg 1$, confirming the existence of the I regime. However, when $h_{min}$ has fallen to $\approx 0.03$, $Re_{local} \ll 1$, which clearly demonstrates that the dynamics has entered the newly discovered intermediate V regime. Finally, as the filament asymptotically approaches breakup, i.e., for values of $h_{min} \approx 10^{-3}$ or smaller, $Re_{local} \sim 1$, demonstrating that near the singularity, all three forces (*viz.*, inertial, viscous, and capillary) balance each other and the

dynamics lies in the IV regime. To confirm the correctness of these computationally made predictions, dripping experiments have been carried out with two liquids of $Oh = 0.23$ and $Oh = 0.55$. For the former, Fig. 2*C* shows the transition from the initial I regime to the intermediate V regime, with the latter regime lasting nearly over two decades in $h_{min}$. When $Oh = 0.23$, it is not possible to observe the transition from the V regime to the final IV regime because that transition occurs for neck radii smaller than a micrometer, which is the lower limit of length scales that can be imaged using visible light. The experimental results for $Oh = 0.55$ depicted in Fig. 2*D*, on the other hand, do show the transition to the final IV regime, albeit with an intermediate V regime of much shorter duration.
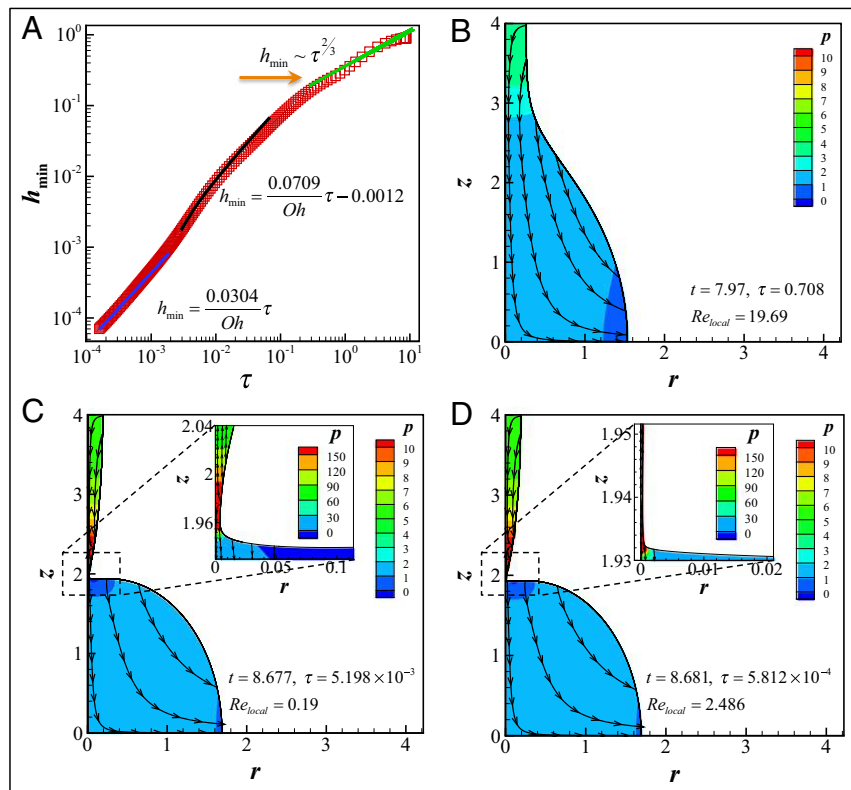
**Fig. 3.** Simulation results when $Oh = 0.07$ highlight the formation of a stagnation zone within the filament and help explain why the intermediate viscous regime exists. (*A*) Variation of minimum neck radius with time until breakup that shows occurrence of all three regimes and transition from I to IV regime through an intermediate V regime. (See below for the explanation of the arrow.) (*B*) Instantaneous streamlines and pressure contours within the thinning filament when the dynamics lies in the I regime. As shown in the figure, this I regime has a slender geometry (21) rather than a fully developed double-cone structure (23). The legend on the top right identifies contour values of the pressure. At this instant in time, the minimum neck radius is located at $z = \lambda/2 = 4$ and the fluid accelerates as it flows from the neck to the swell. (*C*) Instantaneous streamlines and pressure contours in the filament at a later time than in *B* where the acceleration of the fluid has resulted in shifting of the neck from the top end of the domain ($z = 4$) to a location between the two ends ($0 < z < 4$). The time and minimum filament radius when this shift commences is identified by the arrow in *A*. (*Inset*) A new stagnation zone has formed away from the two ends, resulting in a region of reversed flow and the slowing down of the flow in the vicinity of the new minimum in filament radius. (*D*) The stagnation zone persists but because of the large capillary pressures that develop as the neck continues to thin, fluid is once more accelerated as it flows away from the neck. Thus, inertial forces come into play again and compete with viscous and capillary forces in setting the final fate of the filament.

Having demonstrated the existence of the intermediate V regime, we now turn our attention to understanding the reason for its occurrence, which is facilitated by examining flow fields within thinning filaments. To do so, we turn our attention to a filament of $Oh = 0.07$ which, as shown in Fig. 3*A*, clearly depicts the existence of all three scaling regimes. The instantaneous streamlines and pressure contours at three different times when the dynamics lies in each of these three regimes are shown in Fig. 3 *B–D* over $0 \le z \le \lambda/2 \equiv 4$. At early times, the minimum in the filament radius is located at $z = \lambda/2 \equiv 4$, i.e., halfway between two swells, one located at $z = 0$ and the other at $z = \lambda \equiv 8$ (Fig. 3*B*). As the filament continues to thin, the fluid accelerates as it flows from the neck, where pressure is highest, toward the two swells, where pressure is lowest. On account of this effect, which is attributable to finite fluid inertia (20, 22), the filament begins to thin fastest at two locations that are located on either side of $z = \lambda/2$. Within the computational domain, this leads to a shift in the minimum radius from the end of the domain ($z = 4$) to its interior, i.e., $z \approx 1.95$. As shown in Fig. 3*C*, the occurrence of this new minimum gives rise to a new stagnation zone in the interior of the domain in the vicinity of which the flow has slowed down considerably and even reversed. This shift in the location of $h_{min}$ and the accompanying slowing down of the flow then takes the dynamics into the V regime. Although the new stagnation zone persists for some time, the filament does not break while in the

V regime. The capillary pressure which continues to rise as the filament continues to thin accelerates fluid out of the thinning neck and causes inertia to become significant once again, thereby taking the filament into the IV regime. Hence, with the simulation and experimental results shown in Figs. 2 and 3, the thinning and breakup dynamics of slightly viscous filaments for which $Oh < 1$ are seen to exhibit I to V to IV scaling as $\tau \to 0$. Furthermore, these results at long last shed light on the reason for the delay in the transition to the final IV regime that had remained perplexing and unexplained for over a decade.

Having clarified the heretofore inadequately understood thinning dynamics of slightly viscous fluids of $Oh < 1$, we next show that highly viscous fluids of $Oh > 1$ exhibit even more subtle behavior during capillary thinning. Fig. 4 shows results of simulations and experiments for a fluid of $Oh = 1.81$. As expected, both simulations (Fig. 4*A*) and experiments (Fig. 4*B*) reveal that the initial and final scaling regimes are the V and IV regimes. Conventional wisdom dictates that the transition from the V to the IV regime should occur when $h_{min} \sim Oh^{2/(2\beta-1)} = 0.162$, which is contradicted by both simulations and experiments. The simulations show (Fig. 4*A*), and experiments confirm (Fig. 4*B*), that there exists an intermediate I regime that follows the initial V regime. Local Reynolds number calculations near the pinch point from the simulations are yet even more revealing (Fig. 4*C*): they show the existence of an intermediate V regime that lies
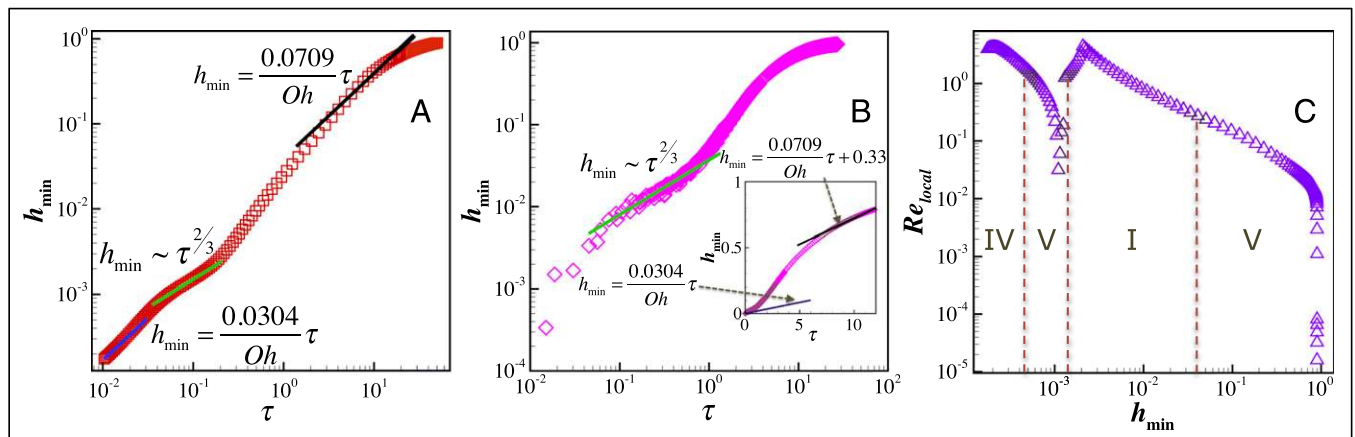
**Fig. 4.** Simulations and experiments demonstrating the existence of several intermediate regimes between the initial viscous regime and the final IV regime for a highly viscous fluid of $Oh = 1.81$. (*A*) Computations show that as the filament thins, the dynamics transitions from an initial V regime to the final IV regime through an intermediate I regime (but see *C*). (*B*) Experiments accord with the predictions from simulations and exhibit the same transition dynamics. (*C*) However, local Reynolds number calculations from the simulations reveal more information about the transitions. Whereas the initial V, intermediate I, and final IV regimes are confirmed from the computed variation of $Re_{local}$ with $h_{min}$, this analysis also indicates the existence for a very short time of an intermediate V regime after the I regime.

between the intermediate I and the final IV regime. Therefore, according to Fig. 4, the capillary thinning of highly viscous filaments for which $Oh > 1$ is seen to transition from V to I to V to IV regimes as $\tau \to 0$. Furthermore, it is worth noting that Fig. 4*A* depicts, to our knowledge, the first demonstration by simulation of the transition from an initial V regime to the final IV regime.

In conclusion, our analysis provides, to our knowledge, the first correct trajectories in the phase space of $(h_{min}, Re_{local})$ that are taken by filaments as they undergo capillary pinching. A particularly interesting finding is that the dynamics cannot reach the asymptotic universal IV regime directly from the I regime without passing through an intermediate transient V regime even though this latter regime may be very short-lived. The presence of the intermediate V regime indicates that even for a low-viscosity fluid, at some stage viscous force (along with capillary force) will dominate the dynamics during filament thinning and breakup. The existence of intermediate regimes has several practical implications as occurrence of slender threads that pinch symmetrically at their midpoints is associated with breakup of highly viscous filaments undergoing creeping flow, whereas occurrence of satellites is associated with inviscid fluids (20, 23, 24, 30). Therefore, the presence of the intermediate I regime makes plain that a visible satellite drop may form even during breakup of highly viscous filaments that reach the IV regime for values of $h_{min}$ below the limit set by visible light. Additionally, the existence of multiple regime transitions before a filament enters the final IV regime helps explain why it has heretofore proven difficult to observe this regime during pinch-off of highly viscous filaments.

The unexpected findings of this work raise a number of questions. Two issues that have not been addressed here are that the amount of time spent by filaments in each regime remains unclear and that similar transitions that may take place during capillary pinching of complex fluids (29, 30) remain unexplored. Moreover, it is well known that there are a number of other free-surface flows that exhibit finite time singularities. Chief among these is the coalescence singularity that arises when two drops are just allowed to touch and then merge into one (31). Whether transitions of the sort uncovered in this work exist in problems like coalescence are worthy topics for future study and may help explain why it took over a decade to uncover the true asymptotic regime of coalescence (31, 32).

## Materials and Methods

**Drop Formation from a Tube and Filament Thinning.** Dynamics of formation of drops of an incompressible Newtonian fluid from a tube at constant flow rate $Q$ is governed by three dimensionless groups (33): Ohnesorge number $Oh = \mu/\sqrt{\rho R \sigma}$, which is the ratio of viscous force to the square root of the product of surface tension and inertial forces; gravitational Bond number $G = \rho g R^2/\sigma$, which is the ratio of gravitational to surface tension force; and Weber number $We = \rho U^2 R/\sigma$ where $U = Q/(\pi R^2)$, which is the ratio of inertial to surface tension force. If the drops are formed quasi-statically so that $We \ll 1$, the dynamics is independent of $We$ (9, 33). Once the filaments shown in Fig. 1*C* become sufficiently thin, the dynamics in the vicinity of the location where filament radius is smallest is also independent of $G$. Therefore, it is both convenient and sufficient to study filament pinch-off in the setup shown in Fig. 1*D* where attention is focused on the time evolution and breakup of an initially cylindrical filament of radius $R$ that is subjected to an axially periodic perturbation of wavelength $\lambda$. The capillary thinning of an idealized filament is governed by three dimensionless groups: the Ohnesorge number $Oh = \mu/\sqrt{\rho R \sigma}$, dimensionless wavelength $\lambda/R$, and dimensionless perturbation amplitude. The latter two parameters must have appropriate values to cause instability (29, 34, 35) but have no effect whatsoever on the dynamics near the singularity.

**Scaling Theories of Pinch-Off.** For filaments of incompressible Newtonian fluids, three theories have been developed to describe the dynamics in the pinching zone (Fig. 1*B*), i.e., the vicinity of the pinch-off singularity $(r = 0, z = z_0)$, where $(r, z)$ are the radial and axial coordinates in a cylindrical coordinate system based along the filament axis and $z_0$ is the axial location where the filament will pinch off. If the effect of viscosity can be neglected and the fluid can be treated as inviscid, i.e., $Oh = 0$, thinning and pinching occur in an inertial (I) or inviscid or potential flow regime (21–23) where inertial and capillary forces balance, and the radial and axial distances and the axial velocity scale with time measured to breakup as $h/R \sim z'/R \sim \tau^{2/3}$, $v/v_c \sim \tau^{-1/3}$. Here, $r = h(z, t)$ is the shape function that prescribes the filament profile, $t$ is time, $z' = z - z_0$ is the length scale of the neck, $\tau = (t_b - t)/t_c$, where $t_b$ is the breakup time and $t_c$ is characteristic time so that $\tau$ is the dimensionless time to breakup, $v$ is the axial velocity, and $v_c$ is characteristic velocity. In the I regime, $t_c \equiv t_I = \sqrt{\rho R^3/\sigma}$ is the inertial-capillary time $t_I$ and $v_c = R/t_c = \sqrt{\sigma/\rho R}$. Real fluids, however, have finite viscosity no matter how small its value. Hence, using these scales, one can calculate an instantaneous Reynolds number $Re(t)$ that applies during thinning of a slightly viscous filament $Oh \ll 1$ as $Re(t) \equiv \rho z' v/\mu \sim \tau^{1/3}/Oh$ (36).

Similarly, if the effect of viscosity is dominant and inertia is negligible so that $Oh = \infty$, thinning and pinching occur in a viscous (V) or Stokes regime (24) where viscous and capillary forces balance, and the radial and axial distances and the axial velocity scale with time measured to breakup as $h/R \sim \tau$, $z'/R \sim \tau^\beta$, $v/v_c \sim \tau^{\beta-1}$, where $\beta = 0.175$. In the V regime, $t_c \equiv t_V = \mu R/\sigma$ is the viscous-capillary time $t_V$ and $v_c = R/t_c = \sigma/\mu$. With these

scales, one can calculate an instantaneous Reynolds number $Re(t)$ that applies during thinning of a highly viscous filament $Oh \gg 1$ as $Re(t) \equiv \rho z' v / \mu \sim \tau^{2\beta-1}/Oh^2$ (36).

Lastly, under the assumption that all three forces, i.e., inertial, viscous, and capillary, remain in a balance as the filament thins and pinches off, Eggers (25) has shown that $h/l_\mu \sim \tau$, $z'/l_\mu \sim \tau^{1/2}$, $v/v_c \sim \tau^{-1/2}$. In this IV regime, $t_c \equiv t_\mu \equiv \mu^3/\rho\sigma^2$ is the viscous time, $l_\mu \equiv \mu^2/\rho\sigma$ is the viscous length, and $v_c = l_\mu/t_\mu = \sigma/\mu$. In this regime, $Re(t) \sim 1$.

**Simulations.** The dynamics of pinch-off of Newtonian filaments is governed by the continuity and Navier–Stokes equations. Because the filament is axisymmetric and subjected to an axially periodic perturbation of wavelength $\lambda$, the domain consists of the 2D region that is bounded by the free surface $S(t)$, the axis of symmetry $r = 0$, and two horizontal planes of symmetry located at $z = 0$ and $z = \lambda/2$, as shown in Fig. 1D. The governing equations are solved subject to symmetry boundary conditions along the axis of symmetry and on the two planes of symmetry, and kinematic and traction boundary conditions along $S(t)$ (33).

The problem statement is made dimensionless using unperturbed radius as characteristic length $l_c \equiv R$, inertial-capillary time as characteristic time $t_c \equiv t_I$, and the ratio of the previous scales as characteristic velocity $v_c \equiv R/t_c$. Different scales are used for pressure and viscous stress, with $p_c \equiv \sigma/R$ as characteristic pressure and $\tau_c \equiv \mu v_c/R$ as characteristic viscous stress.

This free-boundary problem is solved numerically by a fully implicit method of lines algorithm that uses an arbitrary Lagrangian–Eulerian scheme, the Galerkin/finite-element method (G/FEM) for spatial discretization, and an adaptive finite-difference method (FDM) for time integration. Because of the presence of the free boundary, the interior of the flow domain is discretized by an adaptive elliptic mesh generation algorithm (37). The G/FEM converts the time-dependent system of nonlinear partial differential equations to a system of nonlinear ordinary differential equations (ODEs). Application of the FDM time integration scheme further reduces the system of ODEs to a large system of nonlinear algebraic equations. Finally, this system of equations is solved by Newton's method with an analytically computed Jacobian.

Starting from an initially quiescent state corresponding to a deformed cylinder (Fig. 1D), the dynamics is followed in time $\tilde{t} \equiv t/t_c$ until the dimensionless minimum radius $\tilde{h}_{min} \equiv h_{min}/R$ falls below $10^{-4}$. The last few data points obtained on the variation of $\tilde{h}_{min}$ with $\tilde{t}$ before stopping the simulations are then extrapolated to find the dimensionless breakup time $\tilde{t}_b \equiv t_b/t_c$ at which $\tilde{h}_{min} = 0$. In the body of the paper, results are reported as functions of dimensionless time measured to breakup, $viz.$, $\tilde{\tau} \equiv \tau/t_c = \tilde{t}_b - \tilde{t}$. Results from simulations and experiments are compared with the three scaling theories of pinch-off. In dimensionless form, they are $\tilde{h}_{min} \sim \tilde{\tau}^{2/3}$ (I regime), $\tilde{h}_{min} = 0.0709 \, Oh^{-1} \, \tilde{\tau}$ (V regime), and $\tilde{h}_{min} = 0.0304 \, Oh^{-1} \, \tilde{\tau}$ (IV regime). To simplify the notation, in discussing Figs. 2–4 the tildes are omitted and $h_{min}$ and $\tau$ are understood to denote the dimensionless versions of these quantities.

The relative importance of the underlying forces near the pinch point $h_{min}$ is determined by calculating a local Reynolds number $Re_{local} \equiv (1/Oh)z'v$ from the simulation data. Here, $z' \equiv z|_{1.2h_{min}} - z|_{h_{min}}$ is the difference between $z|_{1.2h_{min}}$—the $z$ coordinate of the free surface where $r = 1.2h_{min}$—and $z|_{h_{min}}$—the $z$ coordinate of the location where the neck radius is a minimum. The local velocity $v$ in $Re_{local}$ is the axial velocity at the free surface at $z|_{1.2h_{min}}$.

1. Eggers J (1997) Nonlinear dynamics and breakup of free-surface flows. *Rev Mod Phys* 69(3):865–929.
2. Basaran OA (2002) Small-scale free surface flows with breakup: Drop formation and emerging applications. *AIChE J* 48:1842–1848.
3. Eggers J, Villermaux E (2008) Physics of liquid jets. *Rep Prog Phys* 71(3):036601.
4. Basaran OA, Gao H, Bhat PP (2013) Nonstandard inkjets. *Annu Rev Fluid Mech* 45:85–113.
5. Castrejón-Pita JR, et al. (2013) Future, opportunities and challenges of inkjet technologies. *Atomization and Sprays* 23:541–565.
6. Ambravaneswaran B, Phillips SD, Basaran OA (2000) Theoretical analysis of a dripping faucet. *Phys Rev Lett* 85(25):5332–5335.
7. Ambravaneswaran B, Subramani HJ, Phillips SD, Basaran OA (2004) Dripping-jetting transitions in a dripping faucet. *Phys Rev Lett* 93(3):034501.
8. Zhang X, Harris MT, Basaran OA (1994) Measurement of dynamic surface tension by a growing drop technique. *J Colloid Interface Sci* 168:47–60.
9. Yildirim OE, Xu Q, Basaran OA (2005) Analysis of the drop weight method. *Phys Fluids* 17(6):062107.
10. Heller MJ (2002) DNA microarray technology: Devices, systems, and applications. *Annu Rev Biomed Eng* 4:129–153.
11. Calvert P (2007) Materials science. Printing cells. *Science* 318(5848):208–209.
12. Ptasinski KJ, Kerkhof PJAM (1992) Electric field driven separations: Phenomena and applications. *Sep Sci Technol* 27:995–1021.
13. Kung CY, Barnes MD, Lermer N, Whitten WB, Ramsey JM (1999) Single-molecule analysis of ultradilute solutions with guided streams of 1-microm water droplets. *Appl Opt* 38(9):1481–1487.
14. Berkland C, Kim K, Pack DW (2001) Fabrication of PLG microspheres with precisely controlled and monodisperse size distributions. *J Control Release* 73(1):59–74.
15. Yeo Y, Chen AU, Basaran OA, Park K (2004) Solvent exchange method: A novel microencapsulation technique using dual microdispensers. *Pharm Res* 21(8):1419–1427.
16. Sirringhaus H, et al. (2000) High-resolution inkjet printing of all-polymer transistor circuits. *Science* 290(5499):2123–2126.
17. Caironi M, Gili E, Sakanoue T, Cheng X, Sirringhaus H (2010) High yield, single droplet electrode arrays for nanoscale printed electronics. *ACS Nano* 4(3):1451–1456.
18. Eggers J (2005) Drop formation-an overview. *Z Angew Math Mech* 85(6):400–410.
19. Villermaux E, Bossa B (2009) Single-drop fragmentation determines size distribution of raindrops. *Nat Phys* 5:697–702.
20. Collins RT, Harris MT, Basaran OA (2007) Breakup of electrified jets. *J Fluid Mech* 588:75–129.
21. Keller JB, Miksis MJ (1983) Surface tension driven flows. *SIAM J Appl Math* 43:268–277.
22. Chen YJ, Steen PH (1997) Dynamics of inviscid capillary breakup: Collapse and pinchoff of a film bridge. *J Fluid Mech* 341:245–267.
23. Day RF, Hinch EJ, Lister JR (1998) Self-similar capillary pinchoff of an inviscid fluid. *Phys Rev Lett* 80:704–707.
24. Papageorgiou DT (1995) On the breakup of viscous liquid threads. *Phys Fluids* 7:1529–1544.
25. Eggers J (1993) Universal pinching of 3D axisymmetric free-surface flow. *Phys Rev Lett* 71(21):3458–3460.
26. Chen AU, Notz PK, Basaran OA (2002) Computational and experimental analysis of pinch-off and scaling. *Phys Rev Lett* 88(17):174501.
27. Rothert A, Richter R, Rehberg I (2001) Transition from symmetric to asymmetric scaling function before drop pinch-off. *Phys Rev Lett* 87(8):084501.
28. Liao YC, Franses EI, Basaran OA (2006) Deformation and breakup of a stretching liquid bridge covered with an insoluble surfactant monolayer. *Phys Fluids* 18(2):022101.
29. Suryo R, Basaran OA (2006) Local dynamics during pinch-off of liquid threads of power law fluids: Scaling analysis and self-similarity. *J Non-Newt Fluid Mech* 138:134–160.
30. Bhat PP, et al. (2010) Formation of beads-on-a-string structures during break-up of viscoelastic filaments. *Nat Phys* 6(8):625–631.
31. Paulsen JD, et al. (2012) The inexorable resistance of inertia determines the initial regime of drop coalescence. *Proc Natl Acad Sci USA* 109(18):6857–6861.
32. Eggers J, Lister JR, Stone HA (1999) Coalescence of liquid drops. *J Fluid Mech* 401:293–310.
33. Wilkes ED, Phillips SD, Basaran OA (1999) Computational and experimental analysis of dynamics of drop formation. *Phys Fluids* 11:3577–3598.
34. Rayleigh L (1879) On the capillary phenomena of jets. *Proc R Soc Lond* 29:71–97.
35. Rayleigh L (1878) On the instability of jets. *Proc Lond Math Soc* 10:4–13.
36. Lister JR, Stone HA (1998) Capillary breakup of a viscous thread surrounded by another viscous fluid. *Phys Fluids* 10:2758–2764.
37. Christodoulou KN, Scriven LE (1992) Discretization of free surface flows and other moving boundary problems. *J Comput Phys* 99:39–55.